ISSN 1063-7761, Journal of Experimental and Theoretical Physics, 2017, Vol. 124, No. 2, pp. 244–250. © Pleiades Publishing, Inc., 2017.
Original Russian Text © I.P. Lokhtin, A.V. Belyaev, G. Ponimatkin, E.Yu. Pronina, G.Kh. Eiyubova, 2017, published in Zhurnal Eksperimental'noi i Teoreticheskoi Fiziki, 2017, Vol. 151, No. 2, pp. 285–292.

On the Possibility of Thermalization of Heavy Mesons in Ultrarelativistic Nuclear Collisions

I. P. Lokhtin[a]*, A. V. Belyaev[a], G. Ponimatkin[b], E. Yu. Pronina[a], and G. Kh. Eiyubova[a]

[a] *Skobeltsyn Institute of Nuclear Physics, Moscow State University, Moscow, 119991 Russia*

[b] *Faculty of Nuclear Sciences and Physical Engineering, Czech Technical University in Prague, Prague, 16636 Czech Republic*

**e-mail: Igor.Lokhtin@cern.ch*

Received August 11, 2016

Abstract—The phenomenological analysis and interpretation of experimental data from RHIC and LHC on the production of J/ψ and D mesons in heavy-ion collisions are performed within the two-component HYDJET++ model including the thermal and hard mechanisms of hadron production. It is shown that the thermal freeze-out of charmed mesons at RHIC energies occurs earlier than the thermal freeze-out of light hadrons (assumingly, simultaneously with chemical freeze-out), which indicates that J/ψ and D mesons are not in kinetic equilibrium with the formed hadronic matter. At the same time, a significant part of D mesons at LHC energies are in kinetic equilibrium with the formed thermalized matter, but J/ψ mesons are still characterized by early freeze-out.

DOI: 10.1134/S1063776117010149

1. INTRODUCTION

Investigation of the properties of subnuclear matter at extremely high energy densities and temperatures, which are reached in ultrarelativistic heavy-ion collisions, is one of the most rapidly developed fields of current nuclear physics. Experimental data on multiple particle production in heavy-ion collisions at RHIC and LHC are consistent with the assumption of the formation of hot strongly interacting matter with hydrodynamic properties ("quark–gluon fluid"), which absorbs high-energy quarks and gluons because of their multiple scattering and energy loss [1–6].

Processes with the production of heavy quarks are among important tools for the diagnostics of hot matter in high-energy nuclear collisions. In particular, it is still unclear whether c quarks are thermalized in the quark–gluon matter (so-called "quark–gluon plasma"), which is assumingly formed at the initial stage of the most central ultrarelativistic heavy-ion collisions [7]. An adequate theoretical description of energy loss mechanisms for heavy quarks in dense matter and a computer model implementation of the corresponding mathematical formalism are necessary to answer this question. Another interesting characteristic of the late stage of heavy-ion collisions is the degree of thermalization of heavy mesons in the hadronic fluid formed after the statistical hadronization of the quark–gluon plasma [8, 9]. Phenomenologically analyzing the SPS data on multiple hadron production in lead–lead ion collisions (experiments with a fixed target at the maximum beam energy of 158 GeV per nucleon), the authors of [10] assumed that the "freeze-out" of momentum spectra of J/ψ mesons occurs at an earlier stage of the reaction than the freeze-out of spectra of light hadrons, which can be due to a larger mass and a smaller cross section for the interaction of charmed mesons. It can be expected that the cross section for interaction of charmed mesons in the hadronic matter (as well as the hadronic fluid density) will increase with the energy of beams (at RHIC and LHC), which can significantly affect their degree of thermalization. It is noteworthy that the situation for mesons containing one (D) or two (J/ψ) valence c quarks can be significantly different. An important component of the simulation of the production of heavy mesons in collisions of relativistic nuclei is the inclusion of both the thermal (soft) and nonthermal (hard) production mechanisms.

In this work, we report the results of a phenomenological analysis of RHIC and LHC data on momentum spectra of J/ψ and D mesons in Au–Au collisions at a c.m. energy of 200 GeV per nucleon pair and in Pb–Pb collisions at a c.m. energy of 2.76 GeV per nucleon pair. Events were simulated within the two-component HYDJET++ Monte Carlo model [11], where the final state of the reaction is a superposition of two independent components, soft hydrodynamic and hard jet. It was shown in previous works that this model describes well various characteristics of the multiple production of inclusive (light) hadrons in heavy ion collisions at the RHIC [11] and LHC [12–15] energies.

2. HYDJET++ MODEL

Multiple hadron production in heavy ion collisions at the RHIC and LHC energies was simulated with a HYDJET++ event generator, where the final state of the reaction is a superposition of two independent components, soft hydrodynamic (processes of production with low transverse momenta, thermal component) and hard jet (processes of production with high transverse momenta, nonthermal component). The dominant mechanism of production of charged mesons in this model is the thermal mechanism implying particle production owing to the statistical hadronization of the quark–gluon plasma. The hard mechanism involves rescattering and energy loss of heavy quarks in the hot quark–gluon matter. The model was described in detail in [11, 16]. The main characteristics of the model, which are important for this study, are briefly as follows.

The hadronic state of the soft component of the HYDJET++ model is simulated with the hydrodynamic parameterization of the freeze-out hypersurface [17, 18]. It is assumed that the chemical composition of a hadronic fireball is fixed in the "chemical freeze-out" stage at a given temperature T. In the general case, the chemical freeze-out stage (when the relation between the numbers of different hadrons ceases to change) and the thermal freeze-out stage (when the momentum distribution of hadrons ceases to change) can be separated in time and can occur at different temperatures $T^{\rm ch}$ and $T^{\rm th}$, respectively (such that $T^{\rm ch} \geq T^{\rm th}$). The thermal production of charmed hadrons is considered in the statistical hadronization approximation [8, 9]. In this case, the distribution of hadrons in the rest frame of a hadronic fluid element has the form

$$f_c(p^{*0};T,\gamma_c) = \frac{\gamma_c^{n_c} g_i}{\exp(p^{*0}/T) \pm 1}, \quad (1)$$

where $p*^0$ is the energy of the hadron in the rest frame of the fluid element, g_i is the spin factor, $\gamma_c \geq 1$ is the charm enhancement factor as compared to the thermal value ("fugacity"), n_c is the number of valence c quarks in the hadron C ($C = D$, J/ψ, Λ_c), and the signs + and – in the denominator correspond to the quantum statistics of fermions and bosons, respectively. The fugacity $\gamma_c \geq 1$ can be considered as a free model parameter or can be determined in terms of the total number of $c\bar{c}$ pairs calculated in the perturbative QCD. The multiplicity of hadrons in each event is simulated according to the Poisson distribution around the mean value $\bar{N}$, which is calculated on the freeze-out hypersurface in the effective thermal volume approximation. For charmed hadrons, we have

$$\overline{N_c} = \rho_c^{\rm eq}(T) V_{\rm eff}, \quad \rho_c^{\rm eq}(T) = \int d^3 p^* f_c(p^{*0};T,\gamma_c). \quad (2)$$

Here, $\rho_c^{\rm eq}(T)$ is the thermal (equilibrium) density of hadrons C at the temperature T and $V_{\rm eff}$ is the total effective volume of hadron emission from the hypersurface of the proper time τ = const. This volume is calculated at a given impact parameter b of a nuclear collision as

$$V_{\rm eff} = \tau \int_0^{2\pi} d\phi \int_0^{R(b,\phi)} \sqrt{1 + \delta(b) \tanh^2 Y_{\rm T}(r,b) \cos 2\phi} \times \cosh Y_{\rm T}(r,b) r dr \int_{\eta_{\min}}^{\eta_{\max}} Y_{\rm L}(\eta) d\eta, \quad (3)$$

where $Y_{\rm L}(\eta)$ and $Y_{\rm T}(r, b)$ are the longitudinal (Gaussian) and transverse (linear) collective rapidity profiles, respectively; $R(b, \phi)$ is the transverse size of the fireball in the azimuthal direction ϕ, and $\delta(b)$ is the momentum anisotropy parameter of the source. The characteristics of stable particles and resonances were taken from the SHARE table [19].

In order to simulate the hard component, the HYDJET++ model involves the PYQUEN (PYthia QUENched) event generator [20], which modifies the characteristics of hard parton jets obtained with the PYTHIA hadronic interaction generator [21]. Radiative and collisional energy loss of hard quarks and gluons is associated with each scattering event in a hydrodynamically expanding medium and interference effects are included in gluon radiation by modifying the radiation spectrum as a function of decreasing temperature T. The radiative energy loss of a massless quark per unit length $dE^{\rm rad}/dl$ is calculated within the BDMPS model [22–24]:

$$\frac{dE^{\rm rad}}{dl} = \frac{2\alpha_{\rm s}\mu_{\rm D}^2 C_R}{\pi L} \int_{\mu_{\rm D}^2\lambda_{\rm g}}^{E} d\omega \left[1 - x + \frac{x^2}{2}\right] \ln|\cos(\omega_1\tau_1)|, \quad (4)$$

where

$$\omega_1 = \sqrt{i\left(1 - x + \frac{C_R}{3}x^2\right)\bar{\kappa}\ln\frac{16}{\bar{\kappa}}}, \quad \bar{\kappa} = \frac{\mu_{\rm D}^2\lambda_{\rm g}}{\omega(1-x)},$$

L is the transverse size of the hot region of the quark–gluon matter, $\lambda_{\rm g}$ is the gluon mean free path, $\tau_1 = L/(2\lambda_{\rm g})$, $x = \omega/E$ is the gluon-carried fraction of the energy of the hard quark, $\alpha_{\rm s}$ is the QCD running coupling constant for $N_{\rm f}$ active quark flavors, $C_R = 4/3$ is the quark color factor, and $\mu_{\rm D}$ is the Debye screening mass. For heavy quarks with the mass m_q, we used the simple generalization of Eq. (4) obtained in the "dead-cone" approximation [25]:

$$\left.\frac{dE}{dl}\right|_{m_q \neq 0} = \frac{1}{(1+(\beta\omega)^{3/2})^2}\left.\frac{dE^{\rm rad}}{dl}\right|_{m_q=0}, \quad (5)$$

where

$$\beta = \left(\frac{\lambda}{\mu_{\rm D}^2}\right)^{1/3}\left(\frac{m_q}{E}\right)^{4/3}.$$

Collisional energy loss per unit length $dE^{\rm col}/dl$ and the elastic scattering cross section $d\sigma/dt$ for the hard quark with the energy E and mass m_q on "thermal" partons with the energy $m_0 \approx 3T \ll E$ are calculated in the limit of high squared transverse momentum transfer t [26–28]:

$$\frac{dE^{\rm col}}{dl} = \frac{1}{4T\lambda\sigma}\int\limits_{\mu_{\rm D}^2}^{t_{\max}} dt\frac{d\sigma}{dt}t, \quad (6)$$

$$\frac{d\sigma}{dt} \approx C\frac{2\pi\alpha_s^2(t)}{t^2}\frac{E^2}{E^2-m_q^2}, \quad (7)$$

where $C = 1$ and 4/9 for gq and qq scatterings, respectively, and the maximum possible momentum transfer is given by the expression

$$t_{\max} = \frac{1}{s}[s-(m_q+m_0)^2][s-(m_q-m_0)^2],$$

where

$$s = 2m_0E + m_0^2 + m_q^2.$$

The evolution of dense matter where hard partons lose the energy is described within one-dimensional hydrodynamics with the production of particles on a certain proper time τ hypersurface [29]. The rescattering intensity within the PYQUEN algorithm is determined primarily by the initial maximum temperature $T_0^{\max}$ of the quark–gluon fireball formed in the overlapping region of colliding ions. The initial temperature $T_0^{\max}(b = 0)$ for central heavy-ion collisions is the input parameter of the model; the initial temperature for noncentral collisions $T_0^{\max}(b)$ is calculated from the condition that the corresponding energy density $\varepsilon_0(b)$ is proportional to the ratio of the nuclear overlapping function to the effective transverse area of the overlapping region. The transverse energy density at each point of the overlapping region is taken to be proportional to the product of two nuclear thickness functions T_A. The number of hard jets (including pairs of heavy quarks) in each event is simulated according to the binomial distribution around the mean value $N_{AA}^{\rm jet}$ defined for a given energy of colliding beams $\sqrt{s}$ and the impact parameter b as

$$\overline{N_{AA}^{\rm jet}}(b,\sqrt{s},p_{\rm T}^{\min}) = \int\limits_{p_{\rm T}^{\min}} dp_{\rm T}^2\int dy\frac{d\sigma_{NN}^{\rm hard}(p_T,\sqrt{s})}{dpT^2dy}$$
$$\times\int\limits_0^{2\pi} d\psi\int\limits_0^{\infty} rdrT_A(r_1)T_A(r_2)S(r_1,r_2,p_T,y). \quad (8)$$

Here, $\sigma_{NN}^{\rm in}(p_{\rm T}, \sqrt{s})$ and $\sigma_{NN}^{\rm hard}(p_{\rm T}, \sqrt{s})/dp_{\rm T}^2dy$ are the total inelastic cross section and differential cross section for hard processes with the transverse momentum transfer $p_{\rm T} > p_{\rm T}^{\min}$ in nucleon–nucleon collisions (calculated within the PYTHIA model), respectively; r_1 and r_2 are the transverse distances from the vertex of the initial hard process to the centers of the first and second nuclei, respectively; and the coefficient $S \leq 1$ presents the nuclear shadowing effect of the initial distribution of partons in nucleons. The accepted approximation implies that partons produced in hard processes with momentum transfers lower than $p_{\rm T}^{\min}$ are involved in the thermalized system; therefore, the products of their hadronization are "automatically" included in the soft component of the event. Thus, the model parameter $p_{\rm T}^{\min}$ determines the contribution of the hard component to the total multiplicity of events.

3. MOMENTUM SPECTRA OF J/ψ AND D MESONS IN GOLD–GOLD COLLISIONS AT RHIC ENERGIES

The input parameters of the HYDJET++ model for gold–gold collisions at an energy of $\sqrt{s_{NN}} = 200$ GeV were chosen [11] by fitting RHIC data on the momentum spectra of inclusive charged hadrons at various centralities of interactions. The parameters important for our study are the chemical and thermal freeze-out temperatures $T^{\rm ch} = 165$ MeV and $T^{\rm th} = 100$ MeV, respectively; the maximum rapidities of the longitudinal and transverse flows $Y_{\rm L}^{\max} = 3.3$ and $Y_{\rm T}^{\max} = 1.1$, respectively; the minimum transverse momentum transfer in initial hard parton–parton scatterings $p_{\rm T}^{\min} = 3.5$ GeV/c; and the maximum initial temperature of the quark–gluon plasma $T_0^{\max} = 300$ MeV. The $p_{\rm T}$ spectra of J/ψ and D^0 mesons simulated with the parameters listed above are shown in Figs. 1 and 2 in comparison with the STAR data [30, 31]. The fugacity $\gamma_c = 7$ was chosen from the condition of the identity of the absolute experimental and simulated yields of inclusive J/ψ mesons. It is seen that simulated spectra (dashed lines) are much harder than the experimental spectra, which possibly indicates that the thermal freeze-out of charmed mesons occurs earlier than that of light hadrons and, correspondingly, the collective rapidity of the former is lower than that of the latter [10]. Under the simplifying assumption (which

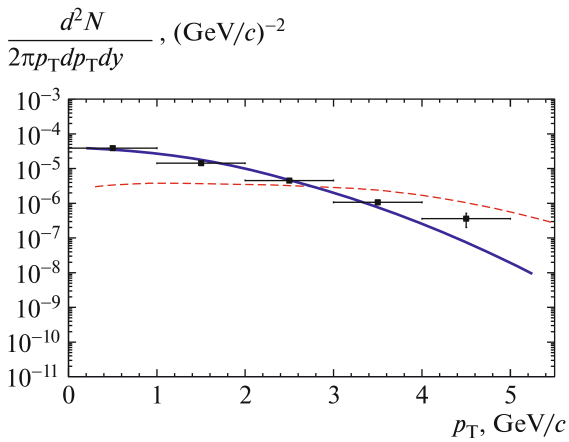

Fig. 1. (Color online) Transverse-momentum distribution of inclusive J/ψ mesons in 20% of the most central Au–Au collisions at the energy $\sqrt{s_{NN}}$ = 200 GeV for the rapidity range $|y| < 1$. The points are STAR experimental data from [30] and the lines are the results of the HYDJET++ simulation with the freeze-out parameters for (dashed curve) inclusive hadrons and (solid curve) "early" thermal freeze-out.

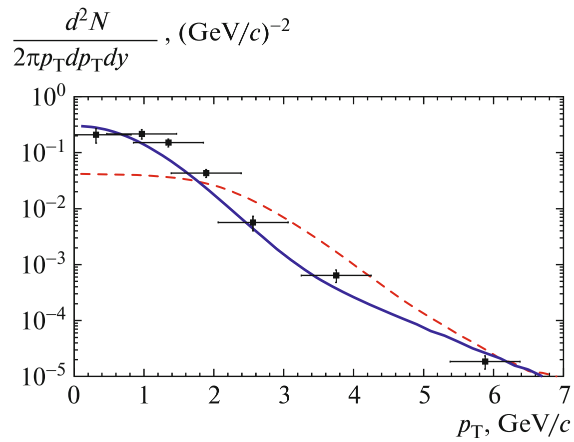

Fig. 2. (Color online) Transverse-momentum distribution of D^0 mesons in 10% of the most central Au–Au collisions at the energy $\sqrt{s_{NN}}$ = 200 GeV for the rapidity range $|y| < 1$. The points are STAR data from [30] and the lines are the results of the HYDJET++ simulation with the freeze-out parameters for (dashed curve) inclusive hadrons and (solid curve) "early" thermal freeze-out.

reduces the number of free parameters) that the thermal freeze-out of charmed mesons occurs at the same temperature, $T^{th} = T^{ch}$ = 165 MeV, the collective rapidities $Y_L^{max} = 1.1$ and $Y_T^{max} = 0.5$ chosen for such a thermal freeze-out hypersurface allow the description of the data for both J/ψ and D^0 mesons (solid lines in Figs. 1 and 2).

Thus, the above model analysis of RHIC data indicates that the thermal freeze-out of charmed mesons occurs earlier than the thermal freeze-out of light hadrons (assumingly, simultaneously with chemical freeze-out), which can be explained by their larger mass and smaller interaction cross section in the hadronic matter. The J/ψ and D mesons are not in kinetic equilibrium with a thermalized medium formed in central collisions of gold ions at RHIC.

4. MOMENTUM SPECTRA AND THE ELLIPTIC FLOW OF J/ψ AND D MESONS IN LEAD–LEAD COLLISIONS AT THE LHC ENERGIES

Various characteristics of multiple production of inclusive hadrons in lead–lead collisions at the LHC energy $\sqrt{s_{NN}}$ = 2.76 TeV were phenomenologically analyzed within the HYDJET++ model in [12–15]. It was shown that the model successfully reproduces data on the momentum spectra [12], anisotropic flow [13], two-particle angular correlations [14], and fluctuations of the elliptic and triangular flows of charged hadrons [15]. The following main input parameters of the model were used: chemical and thermal freeze-out temperatures T^{ch} = 165 MeV and T^{th} = 105 MeV, respectively; maximum rapidities of the longitudinal and transverse flows $Y_L^{max} = 4.5$ and $Y_T^{max} = 1.265$, respectively; the minimum transverse momentum transfer in the initial hard parton–parton scattering p_T^{min} = 8.2 GeV/c; and the maximum initial temperature of the quark–gluon plasma T_0^{max} = 1 GeV. The simulated p_T spectra of J/ψ, $D^{\pm}$, $D^{*\pm}$, and D^0 mesons are shown in Figs. 3 and 4 in comparison with the ALICE data [32, 33]. As in the case of comparison with the STAR data, the fugacity $\gamma_c = 11.5$ was chosen from the condition of identity of the absolute experimental and simulated yields of inclusive J/ψ mesons.

The situation for J/ψ mesons is close to the case of the RHIC energy: the p_T spectrum simulated with the same freeze-out parameters as for inclusive hadrons is harder than the experimental spectrum. Under the assumption of "early" freeze-out $T^{th} = T^{ch}$ = 165 MeV, the data can be described by the model (up to $p_T \approx$ 3.5 GeV/c) with a lower collective rapidity ($Y_L^{max} = 2.3$ and $Y_T^{max} = 0.6$) and a larger contribution of the hard component (p_T^{min} = 3.0 GeV/c). A slight model underestimation of the yield of J/ψ mesons at high transverse momenta (hard component) can be due to the necessity of a special adjustment of the used PYTHIA version to LHC data on the production of J/ψ mesons in proton–proton collisions, but observed discrepancy does not affect the results of the reported analysis.

The situation for D mesons at LHC is qualitatively different as compared to RHIC: their momentum spectra can be described within the HYDJET++

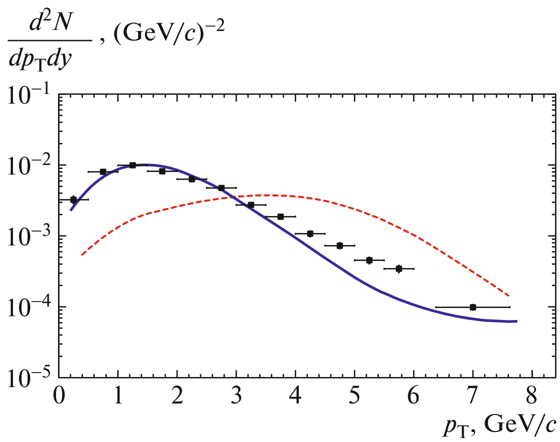

Fig. 3. (Color online) Transverse-momentum distribution of inclusive J/ψ mesons in 20% of the most central Pb–Pb collisions at the energy $\sqrt{s_{NN}}$ = 2.76 TeV for the rapidity range $2.5 < y < 4$. The points are ALICE data from [32] and the lines are the results of the HYDJET++ simulation (the lines mean the same as in Fig. 1).

model with the same freeze-out parameters as for inclusive hadrons. Figure 4 illustrates the comparative contributions of the soft and hard components as functions of the transverse momentum of D mesons. It is seen that the thermal component, which is in kinetic equilibrium with the hadronic matter, dominates up to $p_T \approx 4$ GeV/c. In this case, the data are described up to the highest transverse momentum ($p_T \approx 16$ GeV/c), which indicates that the model of rescattering and energy loss of heavy quarks in hot matter used to generate the hard component in the HYDJET++ model is successive.

An important physical observable characterizing the degree of thermalization of the system of particles formed in relativistic nuclear collisions is an elliptic flow, i.e., the second Fourier harmonic v_2 of the expansion of the azimuthal distribution of particles with respect to the reaction plane. In particular, the observation of a high elliptic flow of inclusive and identified hadrons in heavy-ion collisions at RHIC and LHC indicates the formation of strongly interacting matter with hydrodynamic properties [1–4, 6]. We compared the results of simulation of the elliptic flow of charmed mesons with the ALICE data [34, 35]. Figures 5 and 6 show the momentum dependences of the elliptic flow coefficient v_2 for J/ψ, $D^{\pm}$, $D^{*\pm}$, and D^0 mesons. Good agreement of the simulation results with the experimental data can indicate that assumptions on the freeze-out conditions for heavy mesons and on the relation between the contributions of the soft (thermalized) and hard (nonthermalized) components used in the model are physically justified.

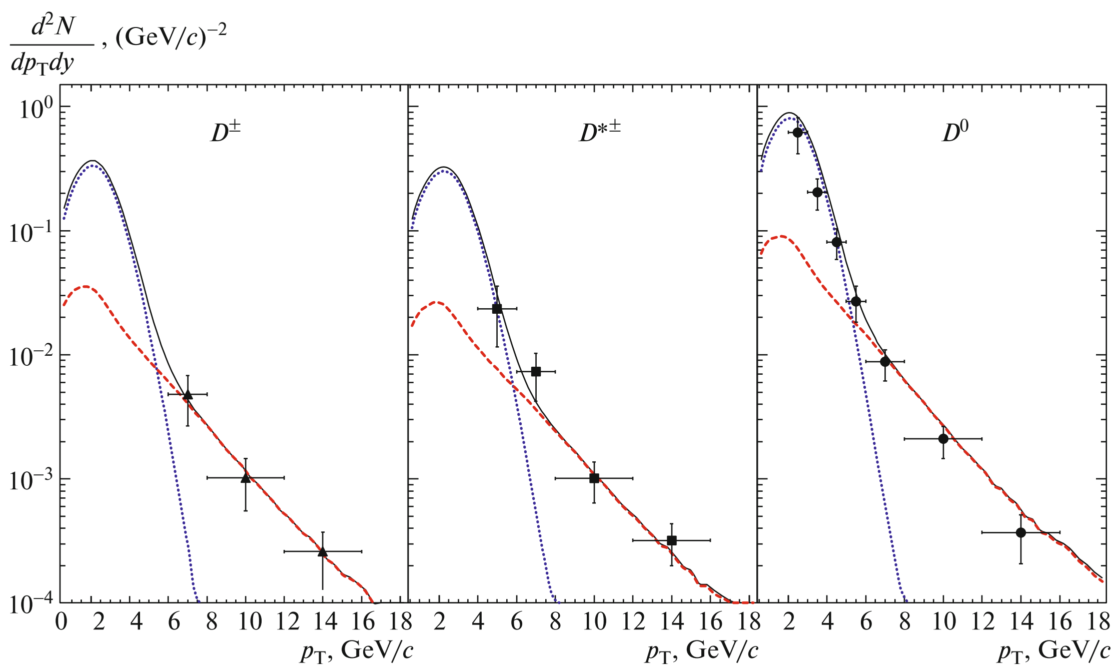

Fig. 4. (Color online) Transverse-momentum distribution of (left panel) $D^{\pm}$, (middle panel) $D^{*\pm}$, and (right panel) D^0 mesons in 20% of the most central Pb–Pb collisions at the energy $\sqrt{s_{NN}}$ = 2.76 TeV for the rapidity range $|y| < 0.5$. The points are ALICE data from [33], the solid curve is the HYDJET++ simulation with the freeze-out parameters for inclusive hadrons, and the dotted and dashed curves are the contributions of the soft and hard components, respectively.

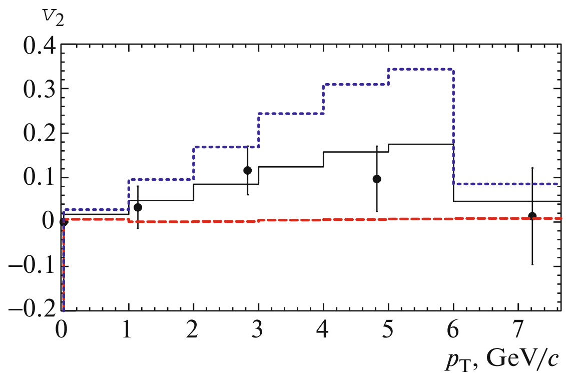

Fig. 5. (Color online) Transverse-momentum dependences of the elliptic flow v_2 of inclusive J/ψ mesons in semicentral Pb–Pb collisions (centrality of 20–40%) at the energy $\sqrt{s_{NN}}$ = 2.76 TeV for the rapidity range $2.5 < y < 4$. The points are ALICE experimental data from [34] and the histograms are the HYDJET++ simulation for "early" thermal freeze-out (the solid, dotted, and dashed histograms mean the same as the respective lines in Fig. 4).

Thus, the model analysis of LHC data shows that the thermal freeze-out of D mesons occurs simultaneously with the thermal freeze-out of light hadrons, whereas the thermal freeze-out of the J/ψ mesons, as at the RHIC energy, occurs earlier than the thermal freeze-out of light hadrons. This effect is possibly caused by an increase in the cross section for the interaction of D mesons at the LHC energy (which becomes comparable with the cross section for the interaction of light hadrons), whereas the cross section for the interaction of J/ψ mesons in the hadronic matter remains significantly smaller.

5. CONCLUSIONS

The model analysis of the data on the production of charmed mesons in heavy ion collisions at the RHIC and LHC energies has been reported. The conditions of freeze-out of the spectra of D and J/ψ mesons and the possibility of their thermalization have been examined. The importance of the nonthermalized component for the description of data has been demonstrated.

It has been shown that the momentum spectra of D and J/ψ mesons in the most central gold–gold collisions at the energy $\sqrt{s_{NN}}$ = 200 GeV can be reproduced within the two-component HYDJET++ model including the hydrodynamic (soft) and jet (hard) components with identical freeze-out parameters. It has been established that the thermal freeze-out of charmed mesons occurs earlier than the thermal freeze-out of light hadrons (assumingly, simultaneously with chemical freeze-out), which can be due to their larger mass and smaller interaction cross section in the hadronic matter. Thus, D and J/ψ mesons at RHIC energies are not in kinetic equilibrium with the formed thermalized hadronic matter.

The momentum spectra and elliptic flow of D and J/ψ mesons in lead–lead collisions at the energy $\sqrt{s_{NN}}$ = 2.76 TeV have been described within the

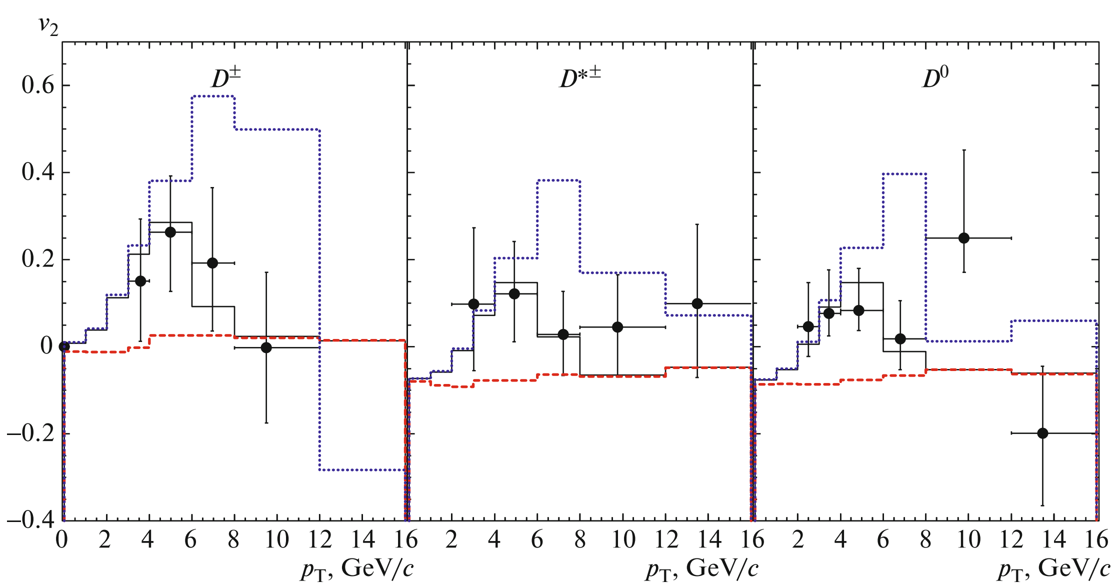

Fig. 6. (Color online) Transverse-momentum dependences of the elliptic flow of (left panel) $D^{\pm}$, (middle panel) $D^{*\pm}$, and (right panel) D^0 mesons in semicentral Pb–Pb collisions (centrality of 30–50%) at the energy $\sqrt{s_{NN}}$ = 2.76 TeV for the rapidity range $|y| < 0.8$. The points are ALICE experimental data from [35] and the histograms are the HYDJET++ simulation with the freeze-out parameters for inclusive hadrons (the solid, dotted, and dashed histograms mean the same as the respective lines in Fig. 4).

HYDJET++ model under the assumption that the thermal freeze-out of D mesons occurs simultaneously with the thermal freeze-out of light hadrons, whereas the thermal freeze-out of J/ψ mesons occurs earlier than the thermal freeze-out of light hadrons. This effect is possibly caused by an increase in the cross section for the interaction of D mesons at the LHC energy (which becomes comparable with the cross section for the interaction of light hadrons), whereas the cross section for the interaction of J/ψ mesons in the hadronic matter remains significantly smaller. Consequently, a significant part of D mesons (up to the transverse momentum $p_T \approx 4$ GeV/c) at LHC, in contrast to RHIC, are in kinetic equilibrium with the formed hadronic matter.

ACKNOWLEDGMENTS

We are grateful to J. Bielcik, V.L. Korotkikh, L.V. Malinina, S.V. Petrushanko, A.M. Snigirev, and E.E. Zabrodin for stimulating discussions. The simulation of the production of heavy mesons at the LHC energies was supported by the Russian Science Foundation (project no. 14-12-00110).

REFERENCES

1. I. Arsene et al. (BRAHMS Collab.), Nucl. Phys. A **757**, 1 (2005).
2. B. B. Back et al. (PHOBOS Collab.), Nucl. Phys. A **757**, 28 (2005).
3. J. Adams et al. (STAR Collab.), Nucl. Phys. A **757**, 102 (2005).
4. K. Adcox et al. (PHENIX Collab.), Nucl. Phys. A **757**, 184 (2005).
5. I. M. Dremin and A. V. Leonidov, Phys. Usp. **53**, 1123 (2010).
6. N. Armesto and E. Scomparin, Eur. Phys. J. P **131**, 52 (2016).
7. S. Cao and S. A. Bass, Phys. Rev. C **84**, 064902 (2011).
8. A. Andronic, P. Braun-Munzinger, K. Redlich, and J. Stachel, Phys. Lett. B **571**, 36 (2003).
9. A. Andronic, P. Braun-Munzinger, K. Redlich, and J. Stachel, Nucl. Phys. A **789**, 334 (2007).
10. K. A. Bugaev, M. Gazdzicki, and M. I. Gorenstein, Phys. Lett. B **523**, 255 (2001).
11. I. P. Lokhtin, L. V. Malinina, S. V. Petrushanko, A. M. Snigirev, I. Arsene, and K. Tywoniuk, Comput. Phys. Commun. **180**, 779 (2009).
12. I. P. Lokhtin, A. V. Belyaev, L. V. Malinina, S. V. Petrushanko, E. P. Rogochnaya, and A. M. Snigirev, Eur. Phys. J. C **72**, 2045 (2012).
13. L. V. Bravina, B. H. Brusheim Johansson, G. Kh. Eyyubova, et al., Eur. Phys. J. C **74**, 2807 (2014).
14. L. V. Bravina, G. Kh. Eyyubova, V. L. Korotkikh, et al., Phys. Rev. C **91**, 064907 (2015).
15. L. V. Bravina, E. S. Fotina, V. L. Korotkikh, et al., Eur. Phys. J. C **75**, 588 (2015).
16. I. P. Lokhtin, L. V. Malinina, S. V. Petrushanko, and A. M. Snigirev, Phys. At. Nucl. **73**, 2139 (2010).
17. N. S. Amelin, R. Lednicky, T. A. Pocheptsov, et al., Phys. Rev. C **74**, 064901 (2006).
18. N. S. Amelin, R. Lednicky, I. P. Lokhtin, et al., Phys. Rev. C **77**, 014903 (2008).
19. G. Torrieri, S. Steinke, W. Broniowski, W. Florkowski, J. Letessier, and J. Rafelski, Comput. Phys. Commun. **167**, 229 (2005).
20. I. P. Lokhtin and A. M. Snigirev, Eur. Phys. J. C **45**, 211 (2006).
21. T. Sjostrand, S. Mrenna, and P. Skands, J. High Energy Phys. **0605**, 026 (2006).
22. R. Baier, Yu. L. Dokshitzer, A. H. Mueller, S. Peigne, and D. Schiff, Nucl. Phys. B **483**, 291 (1997).
23. R. Baier, Yu. L. Dokshitzer, A. H. Mueller, S. Peigne, and D. Schiff, Phys. Rev. C **60**, 064902 (1999).
24. R. Baier, Yu. L. Dokshitzer, A. H. Mueller, and D. Schiff, Phys. Rev. C **64**, 057902 (2001).
25. Yu. L. Dokshitzer and D. Kharzeev, Phys. Lett. B **519**, 199 (2001).
26. J. D. Bjorken, Fermilab Preprint Pub-82/29-THY (1982).
27. E. Braaten and M. Thoma, Phys. Rev. D **44**, 1298 (1991).
28. I. P. Lokhtin and A. M. Snigirev, Eur. Phys. J. C **16**, 527 (2000).
29. J. D. Bjorken, Phys. Rev. D **27**, 140 (1983).
30. L. Adamczyk et al. (STAR Collab.), Phys. Rev. C **90**, 024906 (2014).
31. L. Adamczyk et al. (STAR Collab.), Phys. Rev. Lett. **113**, 142301 (2014).
32. J. Adam et al. (ALICE Collab.), J. High Energy Phys. **1605**, 179 (2016).
33. B. Abelev et al. (ALICE Collab.), J. High Energy Phys. **1209**, 112 (2012).
34. E. Abbas et al. (ALICE Collab.), Phys. Rev. Lett. **111**, 162301 (2013).
35. B. Abelev (ALICE Collab.), Phys. Rev. Lett. **111**, 102301 (2013).

Translated by R. Tyapaev